Biochimica et Biophysica Acta xxx (2015) xxx–xxx

Contents lists available at ScienceDirect

Biochimica et Biophysica Acta

journal homepage: www.elsevier.com/locate/bbagen

Glycomic analysis of gastric carcinoma cells discloses glycans as modulators of RON receptor tyrosine kinase activation in cancer☆

Stefan Mereiter [a,b,c], Ana Magalhães [a,b], Barbara Adamczyk [d], Chunsheng Jin [d], Andreia Almeida [e,f], Lylia Drici [g], Maria Ibáñez-Vea [g], Catarina Gomes [a,b], José A. Ferreira [a,b,h], Luis P. Afonso [i], Lúcio L. Santos [h,j], Martin R. Larsen [g], Daniel Kolarich [e], Niclas G. Karlsson [d], Celso A. Reis [a,b,c,k,*]

[a] I3S — Instituto de Investigação e Inovação em Saúde, University of Porto, Portugal
[b] Institute of Molecular Pathology and Immunology of the University of Porto — IPATIMUP, Porto, Portugal
[c] Institute of Biomedical Sciences of Abel Salazar — ICBAS, University of Porto, Portugal
[d] Department of Medical Biochemistry and Cell Biology, Institute of Biomedicine, Sahlgrenska Academy, University of Gothenburg, Sweden
[e] Department of Biomolecular Systems, Max Planck Institute of Colloids and Interfaces, 14424 Potsdam, Germany
[f] Free University Berlin, Berlin, Germany
[g] Department of Biochemistry and Molecular Biology, University of Southern Denmark, Odense, Denmark
[h] Experimental Pathology and Therapeutics Group, Portuguese Institute of Oncology of Porto, Portugal
[i] Department of Pathology, Portuguese Institute of Oncology of Porto, Portugal
[j] Department of Surgical Oncology, Portuguese Institute of Oncology of Porto, Portugal
[k] Medical Faculty, University of Porto, Portugal

ARTICLE INFO

Article history:
Received 30 October 2015
Received in revised form 18 December 2015
Accepted 19 December 2015
Available online xxxx

Keywords:
ST3GAL4
Sialyl Lewis X (SLeX)
RON
Gastric cancer
Glycome
Sialome

ABSTRACT

Background: Terminal α2-3 and α2-6 sialylation of glycans precludes further chain elongation, leading to the biosynthesis of cancer relevant epitopes such as sialyl-Lewis X (SLe^X). SLe^X overexpression is associated with tumor aggressive phenotype and patients' poor prognosis.
Methods: MKN45 gastric carcinoma cells transfected with the sialyltransferase *ST3GAL4* were established as a model overexpressing sialylated terminal glycans. We have evaluated at the structural level the glycome and the sialoproteome of this gastric cancer cell line applying liquid chromatography and mass spectrometry. We further validated an identified target expression by proximity ligation assay in gastric tumors.
Results: Our results showed that ST3GAL4 overexpression leads to several glycosylation alterations, including reduced *O*-glycan extension and decreased bisected and increased branched *N*-glycans. A shift from α2-6 towards α2-3 linked sialylated *N*-glycans was also observed. Sialoproteomic analysis further identified 47 proteins with significantly increased sialylated *N*-glycans. These included integrins, insulin receptor, carcinoembryonic antigens and RON receptor tyrosine kinase, which are proteins known to be key players in malignancy. Further analysis of RON confirmed its modification with SLe^X and the concomitant activation. SLe^X and RON co-expression was validated in gastric tumors.
Conclusion: The overexpression of ST3GAL4 interferes with the overall glycophenotype of cancer cells affecting a multitude of key proteins involved in malignancy. Aberrant glycosylation of the RON receptor was shown as an alternative mechanism of oncogenic activation.
General significance: This study provides novel targets and points to an integrative tumor glycomic/proteomic-profiling for gastric cancer patients' stratification. This article is part of a Special Issue entitled Glycans in personalised medicine Guest Editor: Professor Gordan Lauc.

1. Introduction

Even more than four decades after declaring "war" on cancer at least 7 million patients die annually from the consequences of this disease, which represents 15% of all deaths worldwide [1,2]. Gastric cancer is globally the fifth most common cancer with near 1 million cases diagnosed in 2012 [3] and represents the third most common cause of cancer-related death. Due to its usually late diagnosis in already advanced stages it remains difficult to treat even in developed countries. Nowadays, there is

Abbreviations: SLe^a, Sialyl Lewis A; SLe^X, Sialyl Lewis X; PTM, Post-translational modifications; RTK, Receptor tyrosine kinase; IHC, Immunohistochemistry; PLA, Proximity ligation assay; GC, gastric cancer; HILIC-FLD-UPLC, hydrophilic interaction liquid chromatography fluorescence detection ultra-performance liquid chromatography.

☆ This article is part of a Special Issue entitled Glycans in personalised medicine Guest Editor: Professor Gordan Lauc.

* Corresponding author at: Institute of Molecular Pathology and Immunology of the University of Porto — IPATIMUP, Porto, Portugal.
E-mail address: celsor@ipatimup.pt (C.A. Reis).

http://dx.doi.org/10.1016/j.bbagen.2015.12.016
0304-4165/

no specific serological assay for the screening and diagnosis of gastric cancer, and endoscopy remains the gold standard in the clinical practice. However, the SLe[a] glycan antigen CA19-9 is currently used for monitoring gastric cancer patients' response to treatment and recurrence [4,5].

One of the most abundant forms of posttranslational modifications (PTM) of proteins is glycosylation, which is a complex process coordinated by the interplay of numerous glycosyltransferases and glycosidases, resulting in a vast diversity of structures. In cancer the disruption of the glycosylation machinery leads to aberrant expression of short truncated carbohydrate chains, known as cancer-associated simple carbohydrate antigens, and to altered expression of terminal sialylated chains [6,7]. These cancer-associated antigens are detected in different types of carcinomas and are associated with disease prognosis, constituting a pool of potential cancer biomarkers, especially when combined with information on the carrying proteins.

It has been long recognized that each cancer patient is different regarding prognosis, clinical presentation, tumor response and tolerance to treatment. With the constant improvement in sequencing and other large-scale analytical technologies, molecular tumor profiling has become unprecedentedly feasible [8]. This enables the identification of the unique combination of alterations, especially that of well-established cancer-related genes, for each patient and personalize their treatment. This customized attempt of tackling cancer has been on the focus of researchers for a long time, but for many cancer-associated alterations the understanding of the biological consequences and therapy-response implications lags behind [9].

One typical target of the personalized therapy strategies is the inhibition of activated signaling pathways, either by interfering directly with the receptor activation or interrupting the downstream signaling cascade by blocking specific GTPases [10]. Receptors such as EGFR, c-MET and RON (Recepteur d'Origine Nantais) can be targeted by small molecules or monoclonal antibodies that act as inhibitors by blocking ligand binding and signaling or by antibodies that tag tumor cells for immune response [10,11]. For instance, the RON receptor tyrosine kinase (also known as macrophage-stimulating protein receptor (MSPR) or MST1R) is constitutively transcribed in many epithelial cells but commonly shows aberrant activation in various tumors due to overexpression and generation of oncogenic variants. Currently several therapeutic agents and monoclonal antibodies targeting RON are tested in clinical and preclinical phases [12].

Therefore, two main goals in gastric cancer research are the discovery of new biomarkers for early diagnosis [5] and the elucidation of altered mechanisms that can be targeted for the development of novel directed and personalized treatments.

In the present work, we have performed a comprehensive analysis of cellular clones derived from MKN45 gastric carcinoma cells overexpressing the human α2,3-sialyltransferase *ST3GAL4*. The *N*- and *O*-glycomic, sialoproteomic and gene expression analysis were performed using a combination of high-throughput methods which revealed several cancer-associated glycomic alterations and generated a list of 47 putative glycoprotein targets with altered glycosylation in gastric cancer cells. Further characterization of one of the targets, the RON receptor tyrosine kinase, confirmed the altered glycosylation and revealed an increased activation of this oncogene in the gastric cancer cells. Finally, we demonstrate that this altered glycosylation of RON receptor tyrosine kinase occurs in human gastric tumors, showing that glycosylation alterations are an alternative pathway for cancer cells to activate receptors that lead to malignant growth, and which can be targets for personalized therapy in gastric cancer patients.

2. Material and Methods

2.1. Cell culture

The gastric carcinoma cell line MKN45 was obtained from the Japanese Cancer Research Bank (Tsukuba, Japan) and was stably transfected with the full length human *ST3GAL4* gene and the corresponding empty vector pcDNA3.1 (Mock) as previously shown [13]. The cells were grown in monolayer culture in uncoated cell culture flasks or cell culture flasks coated with fibronectin or collagen IV (BD BioCoat, BD Biosciences, Franklin Lakes, NJ). Cells were maintained at 37 °C in an atmosphere of 5% CO_2, in RPMI 1640 GlutaMAX, HEPES medium supplemented with 10% fetal bovine serum (FBS), 1% penicillin-streptomycin and in the presence of 0.5 mg/mL G418 (all from Invitrogen, Waltham, MA). Cell culture medium was replaced every two days.

2.2. Quantitative real-time PCR (RT-PCR)

Total RNA extracts from mock and *ST3GAL4* transfected cell lysates were isolated with TRI Reagent (Sigma-Aldrich, St. Louis, MO) and converted into cDNA using the SuperScript® II Reverse Transcriptase (Invitrogen) according to the manufacturer's protocol. The following primers for ST3GAL4 were used applying the protocol previously described [13]: for5′-cctggtagctttcaaggcaatg-3′; rev5′-cctttcgcacccgcttct-3′. Expression level of 18S rRNA was used for mRNA expression normalization (for5′-cgccgctagaggtgaaattc-3′; rev5′-cattcttggcaaatgctttcg-3′).

2.3. RNA next generation sequencing

Total RNA was extracted as previously described in Section 2.2. The mRNAs of over 20,000 primed targets were sequenced by using Ion AmpliSeq Transcriptome Human Gene Expression Kit. The Ion Chef system was used for templating and the loaded chips sequenced using the Ion Proton System (both from Life Technologies). Sequencing data was automatically transfered to the dedicated Ion Torrent server to generate sequencing reads. Reads quality and trimming was performed using Torrent Server v4.2 before read alignment using TMAP 4.2. The TS plugin CoverageAnalysis v4.2 was used to generate reads count. The sequencing was performed in duplicates and sequence reads were normalized to the total read count.

2.4. Immunofluorescence (IF)

Cells were grown in 15 μ-Chamber 12 well glass slides (IBIDI, Martinsried, Germany) and either fixed with 4% paraformaldehyde (PFA) or cold acetone for 15 and 5 min, respectively. The IF protocol performed was as previously described [13] using the antibodies and dilutions noted in Table 1. Samples were examined under a Zeiss Imager.Z1 Axio fluorescence microscope (Zeiss, Welwyn Garden City, UK). Images were acquired using a Zeiss Axio cam MRm and the AxioVision Release 4.8.1 software.

2.5. Protein and phosphoprotein arrays

Confluent cells were lysed in lysis buffer 17 or 6 (R&D Systems, McKinley Place, MN) supplemented with 1 mM sodium orthovanadate, 1 mM phenylmethanesulfonylfluoride (PMSF) and protease inhibitor cocktail (Roche, Basel, Switzerland). The protein concentrations of lysates were determined by the DC protein assay (BioRad, Hercules, CA) and the recommended total protein amounts were used for the human non-haematopoietic soluble receptor array, human phospho-RTK array kit and human phospho-kinase array (R&D Systems). The array protocols were performed according to manufacturer's instructions.

2.6. Western (WB) and Lectin blotting (LB)

Proteins were obtained from total cell lysates as previously described in Section 2.5. Total lysates were denatured and charged using Laemmli buffer, separated by SDS-PAGE and blotted onto a nitrocellulose membrane (GE Healthcare, Chalfont, UK) in a semi-dry system (BioRad). Membranes were incubated with primary antibodies overnight at 4 °C or with biotinylated lectins for 2 h at room temperature (Table 1). Secondary antibodies or avidin (ABC Standard Kit, Vector

Please cite this article as: S. Mereiter, et al., Glycomic analysis of gastric carcinoma cells discloses glycans as modulators of RON receptor tyrosine kinase activation in cancer, Biochim. Biophys. Acta (2015), http://dx.doi.org/10.1016/j.bbagen.2015.12.016

Laboratories, Burlingame, CA) conjugated with peroxidase were incubated for 1 h at room temperature. Target proteins were revealed by chemiluminescence using the ECL Western blotting detection reagent and films (both from GE Healthcare).

2.7. In situ proximity ligation assay (PLA)

In situ Proximity Ligation Assay (PLA) was performed in acetone fixed cells as described in 2.4 or in paraffin sections from human gastric carcinoma tissues for the detection of co-expression in proximity of SLe^X and RON. PLA was performed adapting the procedure previously described [14]. Duolink II reagents (Olink Bioscience, Uppsala, Sweden) were used according to the manufacture instructions. Paraffin sections were dewaxed, rehydrated, antigen retrieval using sodium citrate buffer (10 mM, pH 6.0) was performed before sections were incubated with blocking solution (Olink Bioscience) for 30 min at 37 °C. Primary antibodies against SLe^X and RON were used in equal concentrations as for IF (Table 1) and incubated overnight at 4 °C. Antibodies conjugated with oligonucleotides were utilized as secondary probes (DUO92001 and DUO92005 from Olink Bioscience). Ligation and amplification were performed at 37 °C for 30 min or 120 min respectively and cell nuclei were visualized by DAPI (Sigma-Aldrich, 0.4 mg/ml). Samples were examined under a Zeiss Imager.Z1 Axio fluorescence microscope (Zeiss, Welwyn Garden City, UK) equipped with DAPI, FITC and Texas Red filters. Proximity ligation assays products are seen as bright red fluorescent dots. Images were acquired using a Zeiss Axio cam MRm and the AxioVision Rel. 4.8 software. The resulting images were modified using ImageJ as follows: background with radius 5 was subtracted from the red channel of the RGB images and a multiply filter of 10 was applied. The result was intensity-scaled to suit printing demands.

2.8. Immunohistochemistry (IHC)

Tissue samples from gastric carcinoma patients were obtained from the archives of the Portuguese Institute of Oncology (IPO), Porto, Portugal. All procedures were performed after patient's written informed consent and approved by the local Ethical committee. All clinicopathological information was obtained from patients' clinical records. Expression of SLe^X and RON were evaluated in 15 cases of human gastric carcinomas (10 cases of intestinal subtype and 5 cases of diffuse subtype according to Lauren's classification [15]). Paraffin sections were dewaxed, rehydrated and antigen retrieval was carried out by microwave treatment in sodium citrate buffer (10 mM, pH 6.0) for 20 min. Endogenous peroxidases were blocked with 3% hydrogen peroxide (H_2O_2) in methanol. Tissue sections were further blocked for 30 min with normal goat serum in PBS with 10% BSA, followed by incubation with primary antibodies against SLe^X and RON (Table 1) overnight at 4 °C. Biotin-labeled secondary antibodies (Dako, Glostrup, Denmark) were applied for 30 min and the ABC kit (Vector Labs, Burlingame, CA) for 30 min. Finally, sections were stained by 3,3′-diaminobenzidine tetrahydrochloride (DAB) and counterstained with Mayers' hematoxylin solution. Slides were examined using a Zeiss Optical Microscope.

2.9. Sample preparation for LC-ESI-MS/MS and HILIC-FLD-UPLC analyses

Frozen cell pellets (10^7 cells) were directly resuspended in 7 M urea, 2 M thiourea, 40 mM Tris, 2% CHAPS, 10 mM DTT and 1% protease inhibitor (Sigma-Aldrich, St. Louis, MO). The cell membranes were disrupted by 10 times 10 sec sonication with 16 amplitudes and 1 minute on ice in between, and subsequent shaking at 4 °C overnight. To reduce the viscosity of the lysates, the DNA was degraded by adding 1 μl benzonase® nuclease (250 units, Sigma-Aldrich) and 30 min incubation at 37 °C. In order to impair refolding of proteins, 25 mM iodoacetamide were added for alkylation during 1 h in the dark. The lysates were centrifuged for 30 min with 14,000 rpm and the supernatants transferred to a fresh tube.

Then, solubilized proteins were concentrated by adding 150 μl of supernatant on a 10 kDa cut-off spinfilter (PALL, Port Washington, NY), spinning down for 5 min with 12,000 x g and washing 3 times with 100 μl 50 mM NH_4HCO_3, pH 8.4. *N*-linked oligosaccharides were released in the spinfilter using 20 μl 50 mM NH_4HCO_3 and PNGase F (5 mU, Prozyme, Hayward, CA) with incubation at 37 °C overnight. Subsequently, the *N*-glycans were collected by washing 3 times with 20 μl H_2O and dried in Speedvac. For UPLC analysis samples were further processed as described below and for LC-ESI-MS/MS analysis samples were reduced with 0.5 M $NaBH_4$, 10 mM NaOH at 50 °C overnight. The *O*-linked glycans were released from retained glycoproteins in spinfilter using reductive β-elimination (0.5 M $NaBH_4$, 50 mM NaOH at 50 °C, 16 h). Reactions were quenched with 1 μl of glacial acetic acid and glycan (both *N*-glycans and *O*-glycans) samples were desalted and dried as previously described [16] and subjected to LC-ESI-MS/MS analysis.

2.10. LC-ESI-MS/MS for N- and O-glycomic analysis

Released glycans were analyzed by LC-ESI-MS/MS using a 10 cm x 250 μm I.D. column, prepared in-house, containing 5 μm porous graphitized carbon (PGC) particles (Thermo Scientific, Waltham, MA). Glycans were eluted using a linear gradient from 0 to 40% acetonitrile in 10 mM NH_4HCO_3 over 40 min at a flow rate of 10 μl/min. The eluted *N*- and *O*-glycans were detected using a LTQ ion trap mass spectrometer (Thermo Scientific) in negative-ion mode with an electrospray voltage of 3.5 kV, capillary voltage of −33.0 V and capillary temperature of 300 °C. Air was used as a sheath gas and mass ranges were defined dependent on the specific structure to be analyzed. The data were processed using the Xcalibur software (version 2.0.7, Thermo Scientific) and manually interpreted from their MS/MS spectra.

2.11. Ultra performance liquid chromatography (UPLC)

Released *N*-glycans were labeled by reductive amination with the fluorophore 2-aminobenzamide (2-AB) (Sigma-Aldrich, St.Louis, MO) with sodium cyanoborohydride in 30% v/v acetic acid in DMSO at 65 °C for 2 h. Excess of 2-AB reagent was removed on Glycoworks HILIC cartridges according to the manufacturer's instructions (Waters, Milford, MA) and then concentrated to dryness in speed-vac.

Hydrophilic interaction liquid chromatography (HILIC) of fluorescently labeled *N*-glycans was carried out on a 1.7 μm BEH glycan column (2.1 mm x 15 mm, Waters, Milford, MA) and analyzed using

Table 1
Antibodies and lectins.

Antibody/lectin	Manufacturer	Type	Dil. for WB	Dil. for IHC/IF	Ref.
KM93; Anti-SLe^X	Millipore, Billerica, MA	Mouse IgM	1:500	1:60	[22]
C-20, Anti-RON	Santa Cruz Biotechnology, Dallas, TX	Rabbit IgG	1:1000	1:60	
Anti-p-RON	Santa Cruz Biotechnology	Rabbit IgG	1:1000	1:60	
SNA, biotinylated	Vector Laboratories, Burlingame, CA	Lectin	1:600		[80]

Please cite this article as: S. Mereiter, et al., Glycomic analysis of gastric carcinoma cells discloses glycans as modulators of RON receptor tyrosine kinase activation in cancer, Biochim. Biophys. Acta (2015), http://dx.doi.org/10.1016/j.bbagen.2015.12.016

Waters ACQUITY UPLC® I-class with fluorescence detection. The column temperature was kept at 40 °C and the flow rate set to 0.561 mL/min using a linear gradient of 50 mM ammonium formate (pH 4.4) against acetonitrile with ammonium formate increasing from 30% to 47% over a 25 min period. An injection volume of 25 μL sample prepared in 70% v/v acetonitrile was used throughout. Fluorescence detection was achieved using excitation and emission wavelengths of 330 nm and 420 nm, respectively.

The 2-AB labeled glycans were digested in 10 μL of 50 mM sodium phosphate, pH 6.0 at 37 °C overnight using sialidase S (4 mU, ProZyme) that releases α2-3 linked non-reducing terminal sialic acids (recombinant sialidase from *Streptococcus pneumoniae*, expressed in *Escherichia coli*) and sialidase A (5 mU, ProZyme) that releases α2-3/6/8 linked non-reducing terminal sialic acid (recombinant gene from *Arthrobacter ureafaciens*, expressed in *Escherichia coli*) to confirm sialic acid linkage. After incubation, enzymes were removed by filtration through a 10 kDa cut-off spinfilter (PALL, Port Washington, NY) and the *N*-glycans were analysed by HILIC-FLD-UPLC. The system was calibrated by running an external standard of 2AB–dextran ladder (2AB–glucose homopolymer, Ludger, Oxfordshire, UK) alongside the sample runs. A fifth-order polynomial distribution curve was fitted to the dextran ladder and used to allocate GU values from retention times (using Empower 3 software from Waters) [17].

2.12. Cell lysis, protein digestion and iTRAQ labeling

Cell pellets were redissolved in ice-cold Na_2CO_3 buffer (0.1 M, pH 11) supplemented with protease inhibitor (Roche complete EDTA free), PhosSTOP phosphatase inhibitor cocktail (Roche) and 10 mM sodium pervanadate on ice. The suspensions were tip probe sonicated for 20 s (amplitude = 50%) twice and incubated at 4 °C for 1 h. The lysates were then centrifuged at 100,000× g for 90 min at 4 °C to separate soluble proteins from membrane proteins (pellet). The pellets were washed with 50 mM triethylammonium bicarbonate (TEAB) to remove any remaining soluble protein. The supernatants containing soluble proteins were concentrated using 10 kDa cutoff Amicon ultra centrifugal filters units (Millipore, Billerica, MA. USA) while membrane fractions were resuspended directly in 6 M urea and 2 M thiourea. Soluble and membrane fractions were both reduced in 10 mM DTT for 30 min and then alkylated in 20 mM IAA for 30 min at room temperature in the dark.

Samples were incubated with endoproteinase Lys-C (Wako, Osaka, Japan) for 2 h (1:100 w/w). Following the incubation, the samples were diluted 8 times with 50 mM TEAB (pH 8) and trypsin was added at a ratio of 1:50 (w/w) and left overnight at room temperature. Trypsin digestion was stopped by the addition of 2% formic acid and then the samples were centrifuged at 14,000× g for 10 min to precipitate any lipids present in the sample. The supernatant was purified using in-house packed staged tips with a mixture of Poros R2 and Oligo R3 reversed phase resins (Applied Biosystem, Foster City, CA, USA). Briefly, a small plug of C18 material (3 M Empore) was inserted in the end of a P200 tip, followed by packing of the stage tip with the resins (resuspended in 100% ACN) by applying gentle air pressure. The acidified samples were loaded onto the micro-column after equilibration of the column with 0.1% trifluoroacetic acid (TFA), washed twice with 0.1% TFA and peptides were eluted with 60% ACN/0.1% TFA. A small amount of purified peptides (1 μl) from each sample was subjected to Qubit assay to determine the concentration, while the remaining samples were dried by vacuum centrifugation. Afterwards, peptides were redissolved in dissolution buffer and a total of 150 μg for each condition was labeled with 4-plex iTRAQ™ (Applied Biosystems, Foster City, CA) as described by the manufacturer. After labeling, the samples were mixed 1:1:1:1 and lyophilized by vacuum centrifugation.

2.13. Sialic acid containing glycopeptide enrichment by TiSH protocol

The method used for sialylated glycopeptides enrichment is a modification of the TiSH protocol [18] described in [19]. Briefly, samples were resuspended in loading buffer (1 M glycolic acid, 80% ACN, 5% TFA) and incubated with TiO_2 beads (GL Sciences, Japan, 10 μm; using a total of 0.6 mg TiO_2 beads per 100 μg of peptides). The supernatant containing the unmodified peptides was carefully separated. The TiO_2 beads were sequentially washed with loading buffer, washing buffer 1 (80% ACN, 1% TFA) and washing buffer 2 (20% ACN, 0.1% TFA), saving the washings with the previous supernatant. The bound peptides were eluted with 1.5% ammonium hydroxide by shaking for

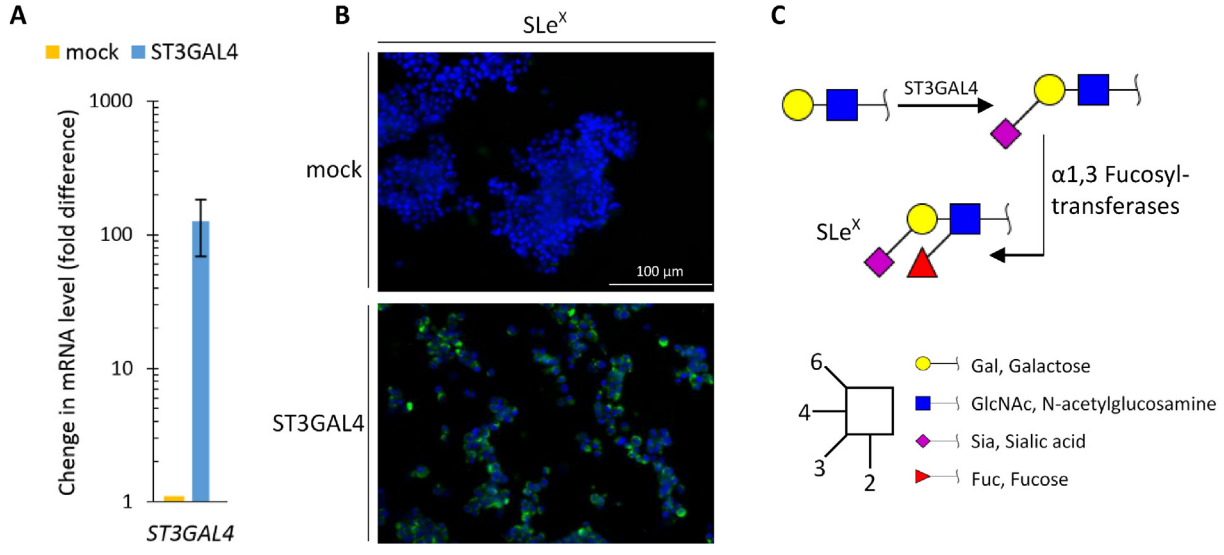

Fig. 1. Gastric carcinoma cell line overexpressing ST3GAL4 shows upregulation of SLe^X expression. A. Relative quantification of *ST3GAL4* mRNA expression using quantitative real-time PCR. MKN45 cells transfected with ST3GAL4 show an approximately 150 times increase when compared with mock transfected MKN45 cells. Values were based on quadruplicates of cell lines. Results are presented as average ± SD. B. Cells that overexpress ST3GAL4 display an increased expression of the SLe^X epitope as shown by immunofluorescence using anti-SLe^X antibody (KM93). C. Depiction of the addition of α2-3 sialic acid to Galβ1-4GlcNAc, which is the major reaction that is catalyzed by the sialyltransferase ST3GAL4 as previously described [18]. The glycan structure Galβ1-4GlcNAc is commonly found in both *N*- and *O*-glycans and is referred to as type 2 chain. This structure can be further fucosylated leading to an increase of the SLe^X glycan epitope.

Please cite this article as: S. Mereiter, et al., Glycomic analysis of gastric carcinoma cells discloses glycans as modulators of RON receptor tyrosine kinase activation in cancer, Biochim. Biophys. Acta (2015), http://dx.doi.org/10.1016/j.bbagen.2015.12.016

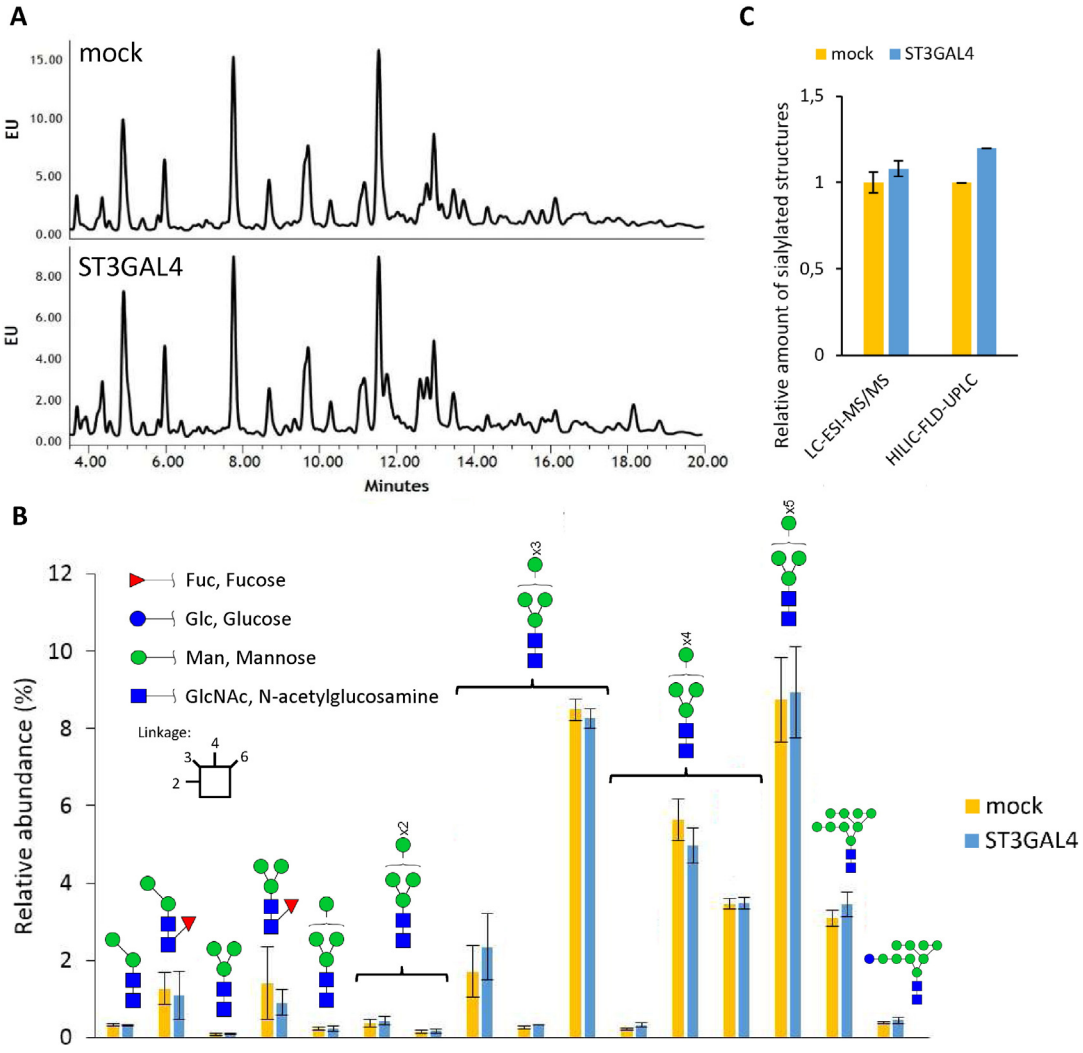

Fig. 2. The overall *N*-glycome of ST3GAL4 overexpressing cells is largely unaltered. A. The quantitative HILIC-FLD-UPLC chromatograms of 2AB labeled N-glycans show highly similar *N*-glycan profiles of *ST3GAL4* transfected and control cell line. EU: Emission unit. B. Relative quantification of high mannose structures reveals that the expression of this group of *N*-glycans is unaffected when compared between ST3GAL4 overexpressing cells and the mock transfected control. *N*-glycans were quantified by evaluating base-peak intensity of extracted ion chromatograms from LC-ESI-MS and were performed in three biological replicates. Values are presented as average ± SD. C. Quantification of the relative amount of sialylated *N*-glycan structures by LC-ESI-MS and HILIC-FLD-UPLC shows no significant increase when comparing sialyltransferase ST3GAL4 overexpressing cells with mock control.

15 min. The eluted fraction containing the phosphopeptides and sialylated glycopeptides was dried by vacuum centrifugation and subjected to an enzymatic deglycosylation in 20 mM TEAB buffer using 500 U of PNGase F (New England Biolabs, Ipswich, MA) and 0.1 U of Sialidase A (Prozyme, Hayward, CA) overnight at 37 °C.

To separate phosphorylated peptides and formerly glycosylated peptides, the samples were subjected to a second TiO_2 enrichment procedure to separate phosphorylated from deglycosylated peptides. The supernatant containing the deglycosylated peptides was saved and the beads were washed with 50% ACN, 0.1% TFA. The washing was added to the supernatant. The deglycosylated fraction was desalted on Oligo R3 staged tip column and dried prior to the HILIC fractionation [19]. All fractions were dried by vacuum centrifugation prior nLC–MS/MS analysis.

2.14. Sialic acid containing glycopeptide analysis by nLC–MS/MS

Samples were resuspended in 6 µL of 0.1% TFA for analysis. Peptides were loaded on an in-house packed Reprosil-Pur C18-AQ (2 cm x 100 µm, 5 µm; Dr. Maisch GmbH, Germany) pre-column and separated on an in-house packed Reprosil-Pur C18-AQ (17 cm x 75 µm, 3 µm; Dr. Maisch GmbH, Germany) column using an Easy-nLC II system (Thermo Scientific, Bremen, Germany) and eluted at a flow of 250 nL/min. Mobile phase was 95% acetonitrile (B) and water (A) both containing 0.1% formic acid. Depending on the samples, gradient was from 1% to 30% solvent B in 80 or 110 min, 30 - 50% B in 10 min, 50 - 100% B in 5 min and 8 min at 100% B. Mass spectrometric analyses were performed in an Orbitrap Fusion Tribrid system (Thermo Scientific, Bremen, Germany). MS scans (400 – 1200 m/z) were acquired in the orbitrap at a resolution of 120000 at 200 m/z for a AGC target of 5 x 10^5 ions and a maximum injection time of 60 ms. Data-dependent HCD MS/MS analysis at top speed of the most intense ions were performed at a resolution of 30,000 at 200 m/z for a AGC target of 5 x 10^4 and a maximum injection time of 150 ms using the quadrupole to isolate the ions and an isolation window of 1.2 m/z, a NCE of 38% and a dynamic exclusion of 20 s.

The raw data were processed and quantified by Proteome Discoverer (version 1.4.1.14, Thermo Scientific) against SwissProt and Uniprot human reference database by using Mascot (v2.3.02, Matrix Science Ltd, London, UK) and Sequest HT, respectively. Database searches were performed using the following parameters: precursor mass tolerance of 10 ppm, product ion mass tolerance of 0.02 Da, 1 missed cleavages for trypsin, carbamidomethylation of Cys and iTRAQ

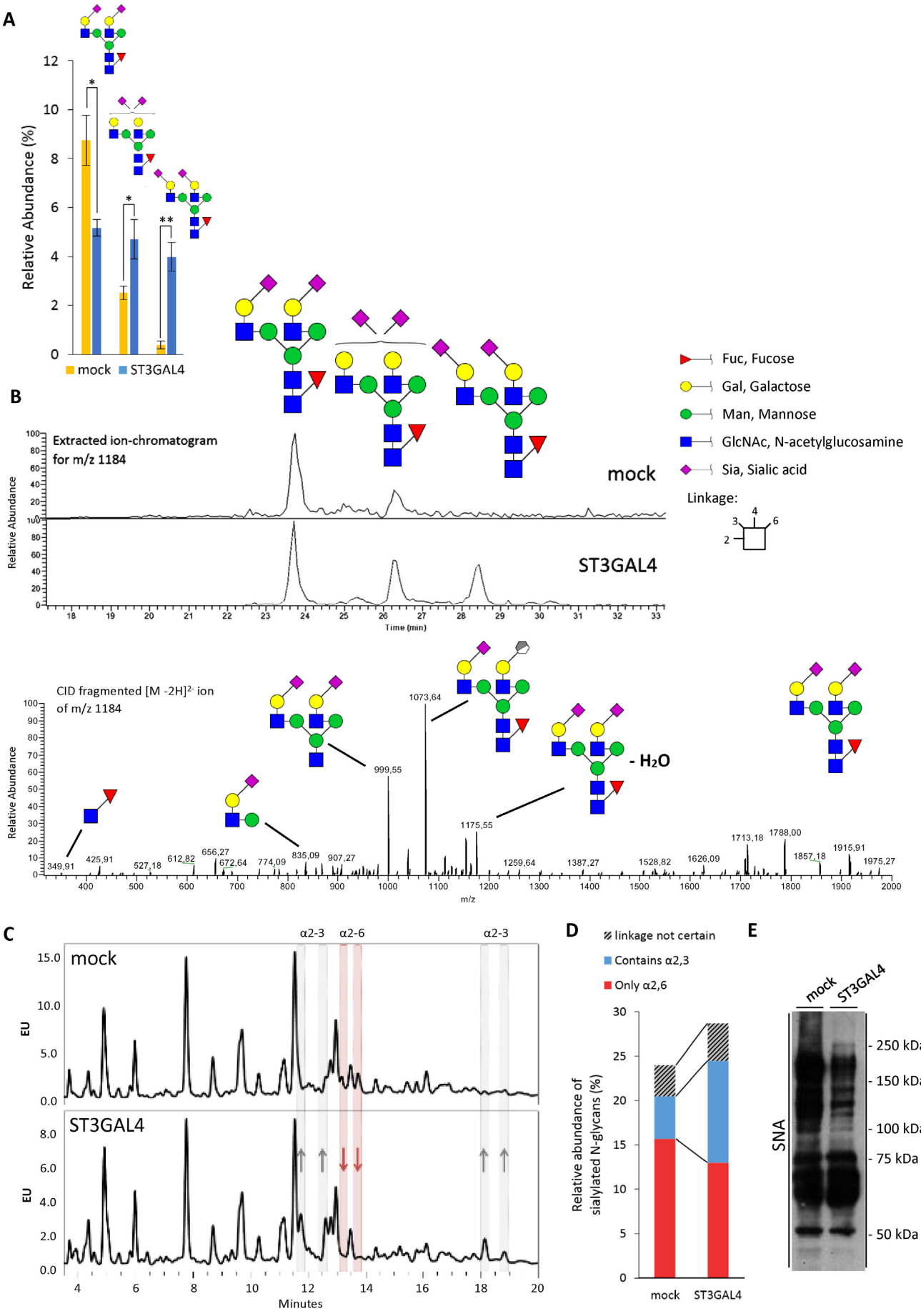

Please cite this article as: S. Mereiter, et al., Glycomic analysis of gastric carcinoma cells discloses glycans as modulators of RON receptor tyrosine kinase activation in cancer, Biochim. Biophys. Acta (2015), http://dx.doi.org/10.1016/j.bbagen.2015.12.016

labelling on protein N-terminal and Lys as fixed modifications, and phosphorylation on S/T/Y and deamidation of Asn as dynamic modifications. The iTRAQ datasets were quantified using the centroid peak intensity with the "reporter ions quantifier" node. Only peptides with up to a q-value of 0.01 (Percolator), Mascot and Sequest HT rank 1, Sequest HT ΔCn of 0.1, cut off value of Mascot score ≥ 18 and a cut-off value of XCorr score for charge states of +1, +2, +3, and +4 higher than 1.5, 2, 2.25 and 2.5, respectively, were considered for further analysis.

2.15. Data normalization and significance analysis

Three biological replicates were analysed and submitted to the statistical analysis. The log2 values of the measured intensities were normalized by the median. Modified peptides were merged with the R Rollup function (http://www.omics.pnl.gov) allowing for one-hit-wonders and using the mean of the normalized intensities for each peptide. Quantification of proteins was obtained by merging the unmodified peptides with the R Rollup function considering at least 2 unique peptides not allowing for one-hit-wonders and using the mean of the intensities. Then the mean over the experimental conditions for each peptide in each replicate was subtracted in order to merge data from different iTRAQ runs. Formerly sialylated glycopeptides containing the consensus motif for N-linked glycosylation (NXS/T/C; where X # P) were normalized based on the protein expression in each of the replicates. Significant up/down-regulations between experimental conditions were calculated allowing a false discovery rate of 0.05. Therefore, we applied combined limma and rank product tests [20], subsequently corrected for multiple testing according to Storey.

Since spontaneous deamidation is frequently observed for asparagine residues, especially when the C-terminal amino acid is glycine (NG), the sites with NGS/T/C are considered as only potential glycosylation. However, in order to reduce the contribution from spontaneous deamidation in the final list, we sort first for the N-linked consensus site (NXS/T/C) and then we filter for proteins that are membrane-associated in order to exclude intracellular proteins that are not N-linked glycosylated.

3. Results

3.1. Overexpression of ST3GAL4 leads to increased expression of SLe^X

The gastric cancer cell line MKN45 shows low expression levels of the sialyltransferase ST3GAL4 and of the terminal glycan epitope sialyl Lewis X (SLe^X) [13]. We have generated clones of MKN45 cells that were stably transfected with the full length *ST3GAL4* resulting in approximately 150 times upregulation of this gene expression (Fig. 1a). ST3GAL4 has been described to be upregulated in the context of gastric cancer and catalyzes the sialylation of Galβ1-3GalNAc on *O*-glycans and of type 2 (Galβ1-4GlcNAcβ-) extensions on both *N*- and *O*-glycans, an intermediate epitope in the biosynthesis of SLe^X [21–23]. As a consequence of the increased expression of ST3GAL4, the terminal glycan epitope SLe^X is overexpressed (Fig. 1). Previous studies on this cell line have demonstrated increased invasive potential both *in vitro* and *in vivo* compared to the mock transfected control cell line [24].

3.2. The N-glycome of ST3GAL4 overexpressing cells is specifically altered in α2-6/3 linked sialic acid content, bisecting and branched structures

To assess the full extent of glycomic alterations in our cell line model we performed a whole *N*-glycomic analysis based on LC-ESI-MS/MS (Table 1 in [25]), to gain semi-quantitative and detailed structural information, and HILIC-FLD-UPLC for quantitative comparisons. The HILIC-FLD-UPLC spectra shows no alteration in the major peaks, which are of high-mannose nature and expectedly unaffected by alterations in sialyltransferase levels. This was confirmed by LC-ESI-MS/MS analysis (Fig. 2a and b). Moreover, the total amount of sialylated structures was not significantly altered (Fig. 2c). It should be noted that the structural analysis revealed also several truncated glycans (Table 1 in [25]) previously described in the MKN45 cell line as free *N*-glycans [26]. Alterations in free *N*-glycans are in conformity with their non-truncated equivalents and are thus not further described in this study.

Despite the overall similarity of the *N*-glycome of cancer cells expressing ST3GAL4 and the control cell line, detailed analysis revealed several specific alterations in the cancer cells expressing ST3GAL4. Our results showed that the sialic acids linked α2-6 were reduced and the α2-3 linked reciprocally increased, indicating a shift of linkage in the *ST3GAL4* transfected cells (Fig. 3). Nevertheless, α2-6 linked sialic acid structures remain a large component of the ST3GAL4 cells' glycome. Since expression levels of sialyltransferases of the ST6 family are unaltered as shown by RNASeq (Supplementary table 1) we hypothesize that the observed isomeric change may be due to competition for the acceptor substrate.

Additionally, bisecting *N*-glycan structures were significantly decreased (Fig. 4). The presence of bisecting *N*-acetylglucosamine excludes the possibility of adding a β1-6 branched arm to the complex *N*-glycan and therefore often inversely correlates with the amount of large branched structures [27,28]. In our cancer cell line model, the amount of large and presumably branched complex *N*-glycans is increased (Fig. 4).

3.3. O-glycomic analysis reveals an increase in truncated O-glycans

Mucin type *O*-glycosylation is commonly altered in cancer with truncation as the most common aberration [29]. MKN45, as a gastric epithelial derived cancer cell line, produces mainly core 2 *O*-glycans [30]. Our analyses showed high amounts of sialylated *O*-glycans in the MKN45 cell line with the majority of structures being decorated with at least one sialic acid (Table 3 in [25]). However, the overexpression of ST3GAL4 leads to an earlier termination by sialylation and thus, to the formation of truncated *O*-glycans (Fig. 5). This is mainly due to the increase in doubly sialylated core 2 structure which accounts for more than 40% of the total *O*-glycan amount in our transfected cells. On the other hand, *O*-glycans composed of more than 2 *N*-acetylhexosamines or hexoses were reduced by approximately 30% (Fig. 5).

3.4. Identification of over 40 glycoproteins with altered glycosylation

The sialoproteomic analysis performed on protein extracts of *ST3GAL4* and mock transfected cells revealed glycoproteins that display aberrant glycosylation. The analysis quantified 1566 unique glycopeptides of which 69 had a significantly altered abundance in sialylated

Fig. 3. Sialylation of *N*-glycans in ST3GAL4 overexpressing cells shows a shift from α2-6 linked towards α2-3 linked. A. Relative quantification of disialylated biantennary structures illustrates the general trend that α2-6 linked sialic acids are reduced whereas α2-3 linked are increased. The quantifications are established by base-peak intensity of extracted ion chromatograms from LC-ESI-MS performed in three biological replicates and presented as average ± SD. Statistical significance was determined by unpaired student's t-test (p-value *<0.05; **<0.01). B. Extracted ion-chromatogram for m/z 1184 shows the relative increase of disialylated biantennary structures with α2-3 linked sialic acids when compared to α2-6 linked. Structures were assigned by a combination of MS^2 spectra (shown below) and α2-3 specific sialidase treatment. C, D. Quantitative HILIC-FLD-UPLC of 2-AB labeled *N*-glycans confirm that α2-3 carrying species are increased and α2-6 are decreased in *ST3GAL4* compared to mock transfected cells. Sialic acid linkage was determined by Sialidase A (releases α2-3,6,8) and Sialidase S (releases α2-3) sialidase treatment experiments. EU: Emission unit. E. *Sambucus nigra* (SNA, binds α2-6 linked sialic acid) lectin blot reveals that especially proteins in the higher molecular mass area (>75kDa) are significantly less decorated with α2,6-linked sialic acid.

Please cite this article as: S. Mereiter, et al., Glycomic analysis of gastric carcinoma cells discloses glycans as modulators of RON receptor tyrosine kinase activation in cancer, Biochim. Biophys. Acta (2015), http://dx.doi.org/10.1016/j.bbagen.2015.12.016

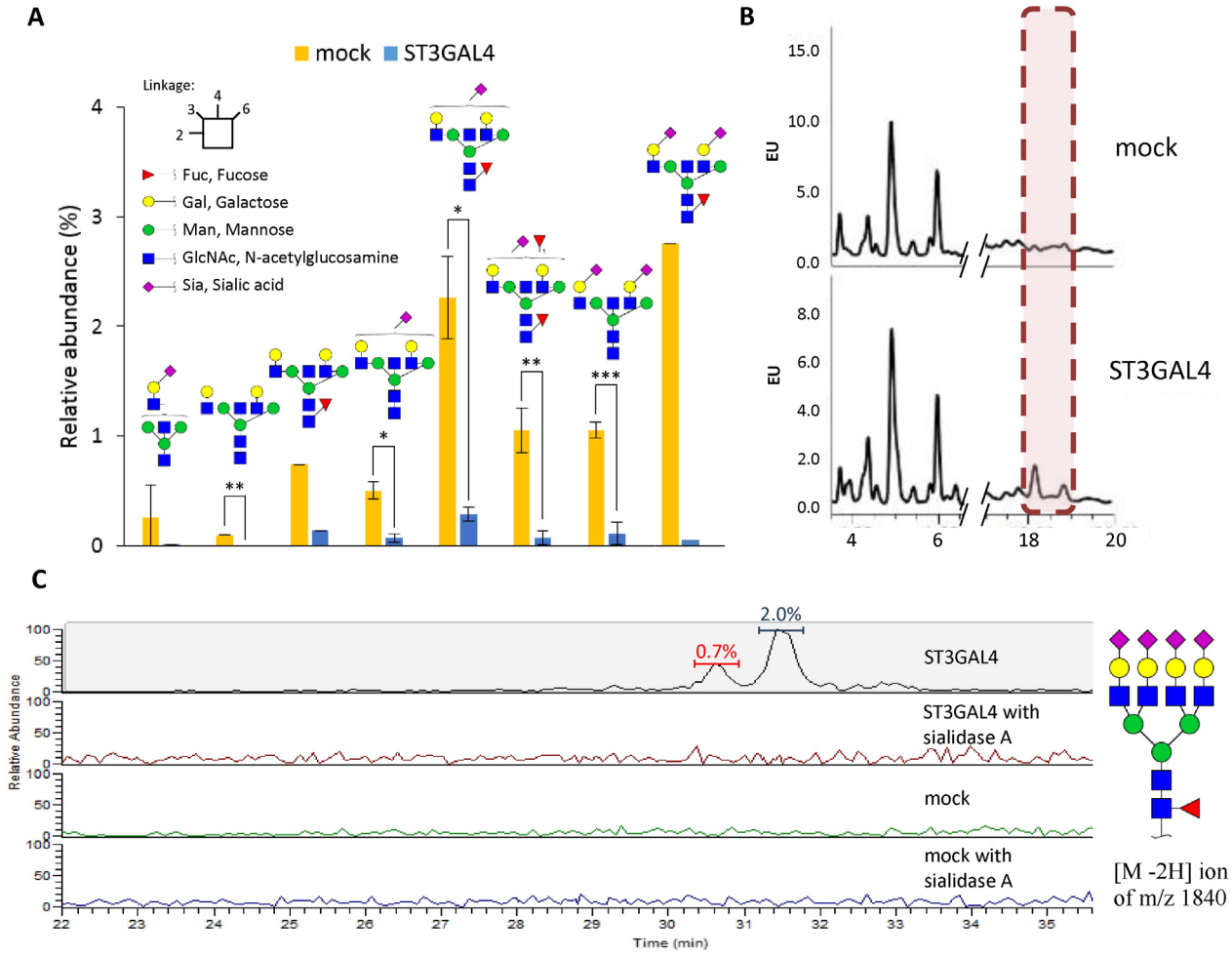

Fig. 4. Bisecting structures are significantly reduced and large branched *N*-glycans are increased in ST3GAL4 overexpressing cells. A. Quantification of relative abundance of bisecting structures shows significant reduction of all examined structures. The glycans were quantified with base-peak intensity of extracted ion chromatograms from LC-ESI-MS performed in three biological replicates. Statistical significance was determined by unpaired student's t-test (p-value *<0.05; **<0.01; ***<0.001). B. The *N*-glycan HILIC-FLD-UPLC data reveals an increase in very large, putative highly branched, α2-3 sialylated *N*-glycans (framed area) in ST3GAL4 overexpressing cells. These structures correspond to approximately 4% of the total *N*-glycome. EU: emission units. C. Core fucosylated, tetrasialylated, tetraantennary structures (depicted on the right side) are very abundant in ST3GAL4 overexpressing cells but are not detectable in the mock control as shown by extracted ion chromatogram of [M–2H] ion of m/z 1840. The two peaks in the upper panel correspond to isomers of the depicted structure. Annotation is based on fragmentation spectra and glycosidase digestion experiments. Relative amount was determined by base-peak intensity and is shown above the corresponding peaks.

N-glycosylation. Of those glycopeptides two showed a decrease in sialylation and the remaining 67 an increase in *ST3GAL4* transfected cells, corresponding to an overall total of 47 glycoproteins (Table 5 and 6 in [25]). Many of the identified glycoproteins have established functions in cellular signaling as either receptors or receptor interacting proteins, in cellular adhesion and migration, or are proteases (Fig. 6). Among the identified glycoproteins, many well characterized targets that are described to be altered in the context of gastric carcinogenesis were found, such as insulin receptor, CEACAM1, CEA, various integrins and RON [12,31–33].

3.5. Activation of altered glycosylated RON receptor tyrosine kinase

Given that the sialoproteomic analysis pointed out a potential alteration of the RON receptor tyrosine kinase glycosylation, we investigated this further, especially since this protein has been shown to be hyperactivated in the context of gastric cancer, contributing in tumorigenesis, malignant progression, angiogenesis, chemoresistance and correlating with bad prognosis [34–38]. Several mechanisms, including overexpression of this receptor and generation of oncogenic variants, have been described that can account for aberrant activation of RON, however, there are cases in which the cause for this abnormal activation remains unknown [38–40]. Comparative analysis between ST3GAL4 overexpressing cells and the mock transfected cells revealed that the expression of RON is unaltered at both RNA (Supplementary table 1) and protein levels (Fig. 7), but shows around 4.5 times increased receptor activation in ST3GAL4 overexpressing cells (Fig. 7a, b), as measured by the increase of phosphorylation of RON. The activated phosphorylated RON protein was observed on the plasma membrane coinciding with the expected localization of fully glycosylated RON (Fig. 7c).

3.6. Altered glycosylation of RON in gastric cancer

In order to confirm the altered glycosylation of RON in the cell line model we used *in situ* proximity ligation assay (PLA). We demonstrated that RON is aberrantly glycosylated carrying the SLe^X epitope in *ST3GAL4* transfected cells (Fig. 8). The localization of RON receptor decorated with SLe^X was observed in the cellular membrane. To assess whether the modification of RON occurs also in gastric carcinoma tissues we screened 15 human gastric tumor samples for the evaluation of the expression of RON and SLe^X. Of these 15 cases, 8 that showed

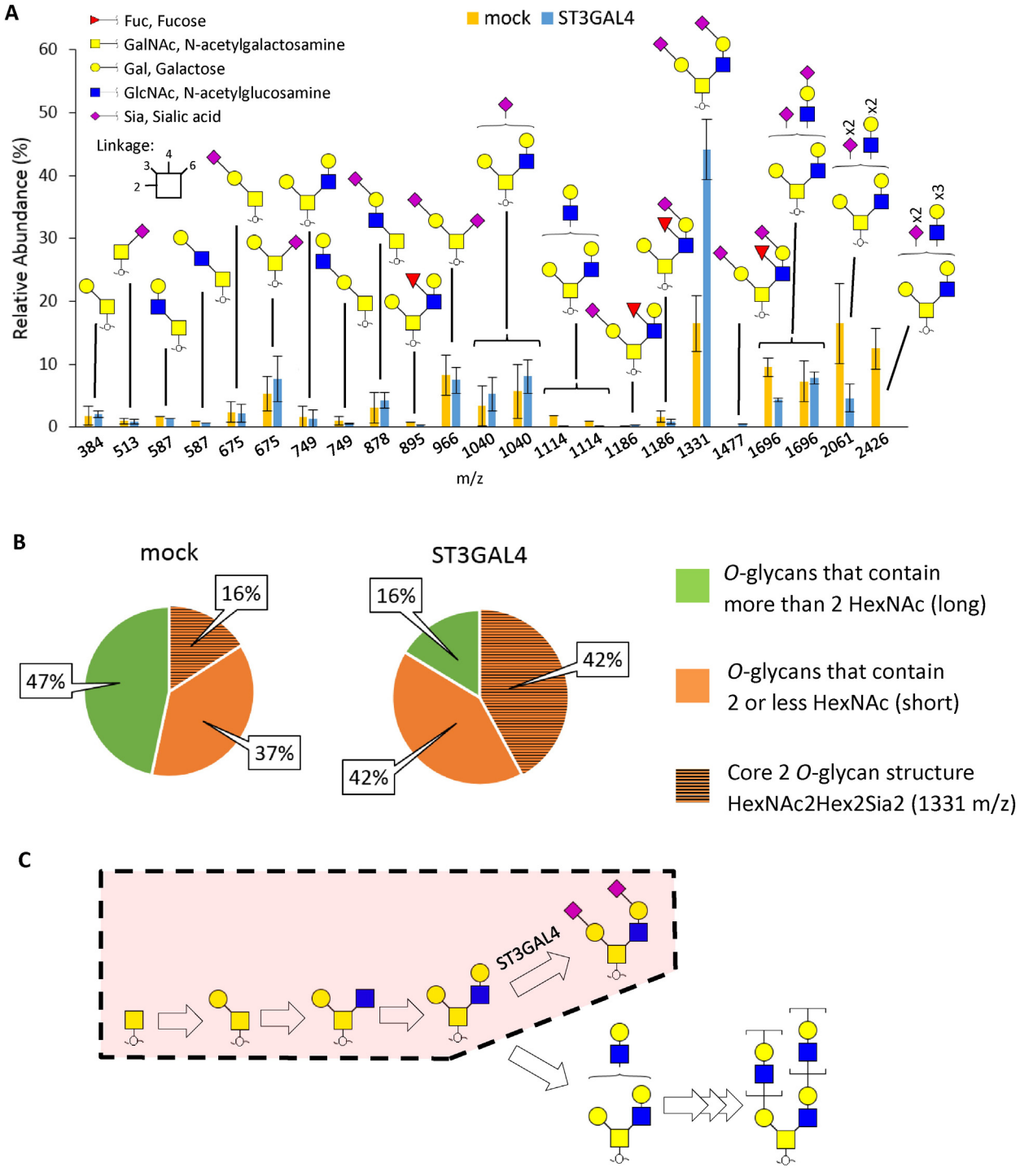

Fig. 5. Increase in disialylated core 2 structures in ST3GAL4 overexpressing cells leads to earlier termination and thus truncation of *O*-glycan structures. A. Relative abundance of all structurally characterized *O*-glycan compounds. Diagram is ordered from left to right by mass. Simple *O*-glycan residues show no significant alteration. Terminated unextended disialylated core 2 structures [M –H] ion of m/z 1331 are significantly increased and as a consequence extended structures are reduced in ST3GAL4 overexpressing cells. The quantifications are established by base-peak intensity of extracted ion chromatograms from LC-ESI-MS performed in three biological replicates and presented as average ± SD. B. Pie-diagram illustrates the approximately equal distribution of short and long *O*-glycans in mock transfected MKN45 cells, and the truncation that is observed in ST3GAL4 overexpressing cells. *O*-glycans with less than or equal 2 HexNAc or Hex were considered short *O*-glycans, structures with 3 or more HexNAcs or Hex were considered long *O*-glycans. The abundance of the simple disialylated core 2 structure (NeuAc2Hex2HexNAc2) is highlighted in dashed orange C. Schematic representation of the impact of ST3GAL4 overexpression on the biosynthesis of *O*-glycan in MKN45. The frame indicates the preferred pathway in the *ST3GAL4* transfected cell line.

expression of both antigens were further analyzed by PLA (Supplementary table 2). All evaluated cases showed PLA positivity signal with 2 cases displaying a high number of signal corresponding to co-expression in proximity of RON and SLe^X. The tumor adjacent mucosa did not show any PLA signal and represents an internal control (Fig. 8).

4. Discussion

The altered glycosylation observed in gastric cancer with overexpression of α2-3 sialylated glycans, including the SLe^X epitope, has long been associated with aggressive features of the disease and poor prognosis for the patients [5,7,41–43]. However, the biological role of

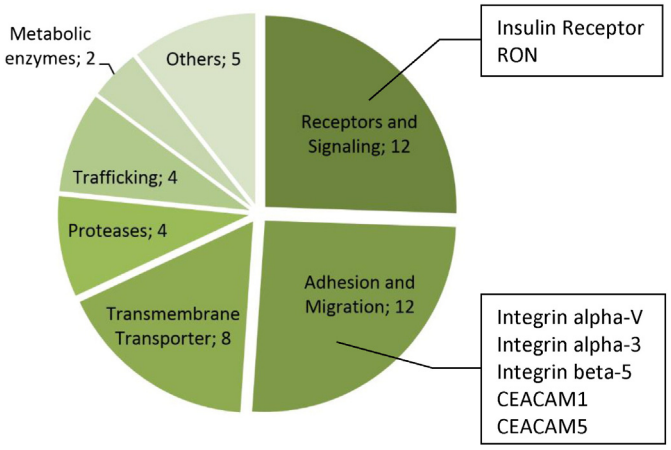

Fig. 6. Representation of the biological functions of the proteins identified with increased sialylation on their N-glycans in *ST3GAL4* transfected cells. Functional clustering reveals that most of the proteins found with increased sialylated N-glycans are involved in signaling, adhesion and migration processes. Remarkably many of these targets have been described to be often altered in gastric cancer. The 47 proteins with significantly increased sialylation were classified according to their main function described in Uniprot (www.uniprot.org).

these sialylated glycans remains to be fully understood. In this study, the detailed molecular characterization of gastric cancer cells displaying altered sialylated terminal glycan structures revealed how these glycosylation modifications can lead to functional changes that confer advantage to cancer cells.

4.1. Glycosylation alterations induced by ST3GAL4 overexpression

The sialyltransferase ST3GAL4, encoded by the *ST3GAL4* gene, catalyzes the addition of α2-3-sialic acid to type 2 extension chains (Galβ1,4GlcNAcβ1-R) generating the precursor of SLe^X [13,21]. In our study we demonstrated that the overexpression of ST3GAL4, in accordance to its substrate specificity, leads to a broad range of glycomic alterations on both *N*- and *O*-glycans. Importantly, ST3GAL4 overexpression induces the expression of SLe^X which has been described to be commonly upregulated in gastric cancer [41,44,45]. Further, we demonstrated for the first time in a gastric cancer context that the upregulation of ST3GAL4, an α2-3 sialyltransferase, not only increases the amount of α2-3 linked sialic acid, but as a consequence, reduces the amount of α2-6-linked sialic acid expressed by the cancer cell, as it has been previously reported in a pancreatic cancer cell line model [46]. The expression levels of other sialyltransferases remained unaltered (Supplementary table 1) supporting the assumption that this linkage-shift is rooted in competition for the same asialylated substrate. Although the general amount of sialylated glycans is described to increase in the context of transformation and malignancy [47,48], it is known that the linkage type is of particular importance. Interestingly, the upregulation of α2-6 sialylation has been shown to increase the adhesion of colon and breast cancer cells to extra cellular matrix components and to reduce the invasive capacity of colon and glioma cancer cell lines [49–51]. Similarly, the increased invasive capacity of ST3GAL4 overexpressing cells previously described [24] could also result from the reduction of α2-6 linked sialic acid modified structures.

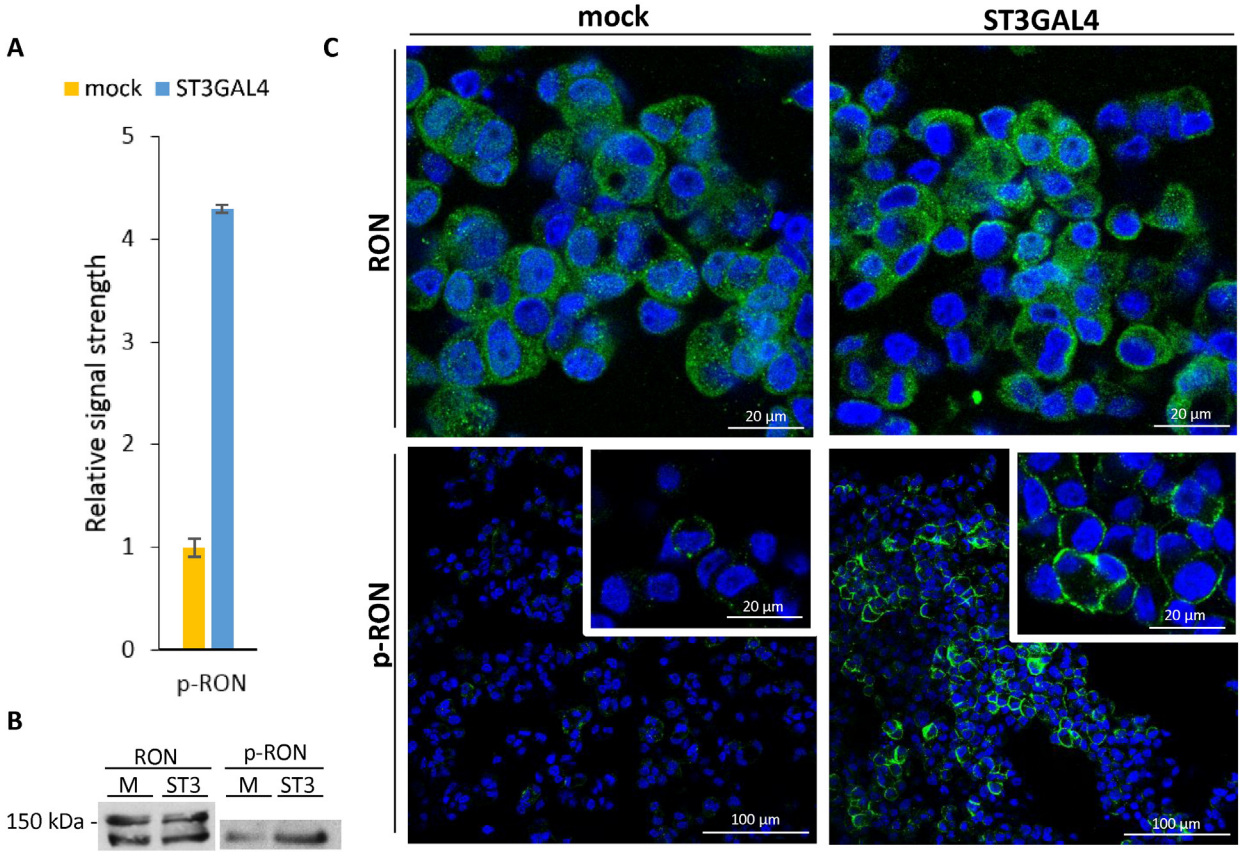

Fig. 7. Receptor tyrosine kinase RON is activated in ST3GAL4 overexpressing cells. A. RON shows approximately 4.5 fold increased activation in ST3GAL4 overexpressing cells as indicated by phospho-RTK array results. The optical density of p-RON signal was measured in duplicates. Average values, with standard deviation are shown. The receptor activation of *ST3GAL4* transfected cells is shown relative to the mock control cells. B. Western blot for RON and phosphorylated RON (p-RON) confirms the increased phosphorylation of RON in ST3GAL4 overexpressing cells and shows no difference in total RON receptor amount. C. Immunofluorescence images of cells stained for RON show cytoplasmic and membrane localization of the receptor with similar amounts for both, *ST3GAL4* transfected and control cell lines. In contrast, activated RON is localized at the plasma membrane and strongly increased in cells overexpressing ST3GAL4.

Please cite this article as: S. Mereiter, et al., Glycomic analysis of gastric carcinoma cells discloses glycans as modulators of RON receptor tyrosine kinase activation in cancer, Biochim. Biophys. Acta (2015), http://dx.doi.org/10.1016/j.bbagen.2015.12.016

Our results also showed an almost complete loss of all bisected *N*-glycan structures in cancer cells overexpressing ST3GAL4. A correlation between sialylation and the activity of GnT-III, the GlcNAc-transferase that leads to the synthesis of bisected *N*-glycans, has to our knowledge never been reported. Sialyltransferases are normally located in the trans-Golgi and the sialylation resembles a capping event for mature complex and hybrid *N*-glycans [52], on the other hand the GnT-III is localized in the medial-Golgi and acts early on the biosynthesis of complex *N*-glycans [53]. It is important to consider that the subcellular localization of glycosyltransferases and the organization of the secretory compartments are often altered in the context of cancer [54] and this may lead to deviations of the conventional sequential biosynthesis pathway. Moreover, it is known that bisected structures are often reduced in malignancy and this reduction is correlated with tumor progression and poorer prognosis [27,55,56]. Our results showed that *N*-glycans from *ST3GAL4* transfected cells display a higher degree of branching resulting in enlargement and increased complexity of structures. In addition, no differences were observed on GnT-V, which is the GlcNAc-transferase that catalyzes the formation of β1-6 branched *N*-glycans, and GnT-III expression levels (Supplementary table 1). These enzymes are known to act mutually exclusive on their common glycan acceptor substrate [28,53,56], and therefore the increased branched *N*-glycans could stem from the reduced amount of bisected structures.

Regarding *O*-glycosylation, we demonstrated that ST3GAL*4* upregulation can also lead to the increased truncation of otherwise elongated *O*-glycans. The accumulation of short truncated *O*-glycans like simple carbohydrate antigens are a common feature of gastrointestinal cancer [57]. Our results show that the biosynthesis of early sialylated core-2 structures preclude further elongation of the *O*-glycan chain.

Our data indicates, for the first time, that several cancer relevant glycomic alterations, such as truncation of *O*-glycans, reduction of bisected *N*-glycans, increase of α2-3 sialylation and branching, might not be independent events but may arise coordinated in gastric cancer. The observed changes were further confirmed in an additional glycomic analysis performed in parallel (Tables 2 and 4 in [25]) [58,59]. These glycophenotypic alterations may result from genetic and epigenetic alterations, as well as from tumor microenvironment modifications, occurring in the cancer context [60–63].

4.2. Target proteins displaying aberrant sialylation and its biological implications

In addition, our results revealed that even though the total amount of sialylated *N*-glycans is not significantly increased, 47 glycoproteins showed significantly increased sialylation in a site specific manner in ST3GAL4 overexpressing cancer cells. Considering that only proteins that are translated into the ER are *N*-glycosylated and that only those proteins that are conveyed through the Golgi-network undergo addition of sialic acids [64], it is not surprising that especially transmembrane proteins were found to be affected by the increased sialylation. Furthermore, an interesting observation is that mainly proteins involved

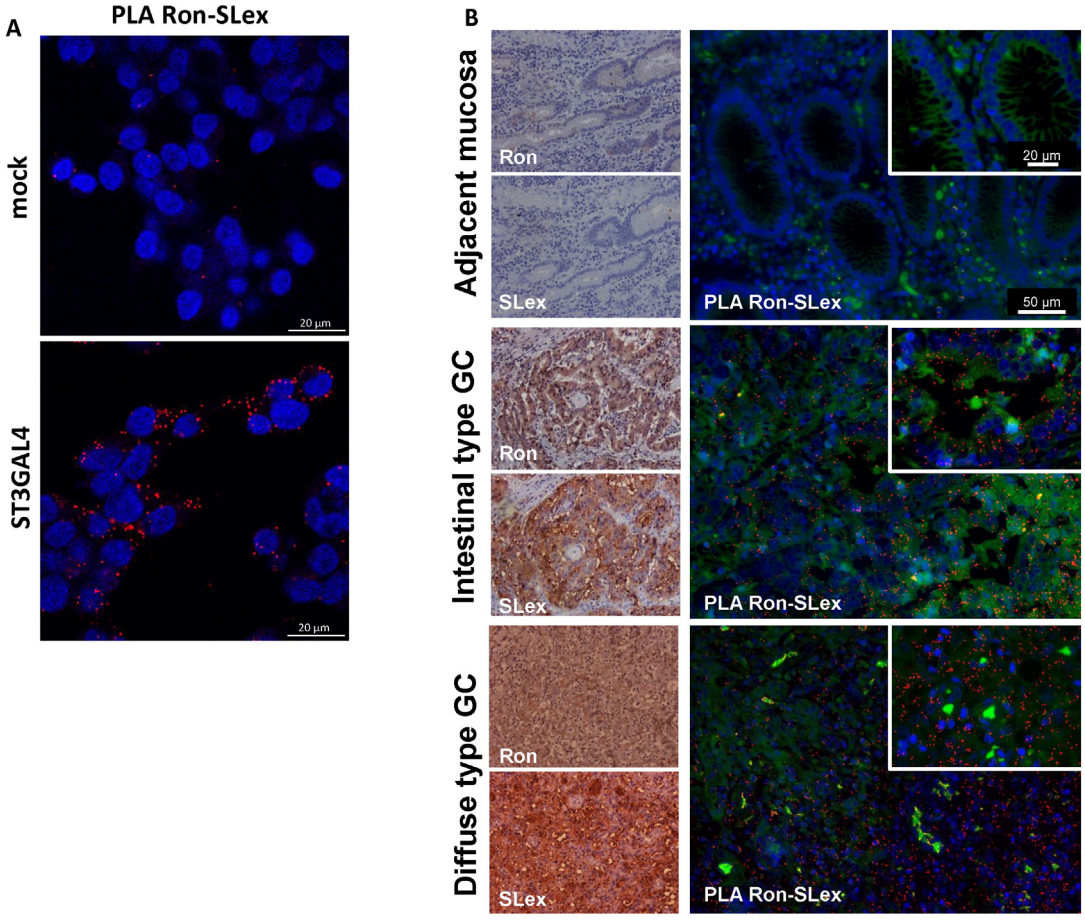

Fig. 8. Receptor tyrosine kinase RON is aberrantly glycosylated with SLe^X in gastric cancer. A. The mock transfected cell line is largely negative in the PLA for RON and SLe^X. On the other hand ST3GAL4 overexpressing cells show strong PLA signal, confirming altered glycosylation of the RON receptor in these cells. The PLA signal is shown in red and nuclei in blue. B. Screening of gastric tumor samples with IHC for RON or SLe^X (left panel) and PLA for RON and SLe^X (right panel). Adjacent mucosa is negative for SLe^X and expresses low level of RON as shown by IHC. The PLA experiment shows no signal in the adjacent mucosa and resembles an internal negative control. The selected cases of intestinal type GC and diffuse type GC are positive for SLe^X and RON. Evaluation of colocalization by PLA reveals that RON is a carrier of SLe^X in gastric carcinomas. The PLA signal is shown in red and nuclei in blue. Tissue autofluoresence has been used to visualize the tissue structure (green).

Please cite this article as: S. Mereiter, et al., Glycomic analysis of gastric carcinoma cells discloses glycans as modulators of RON receptor tyrosine kinase activation in cancer, Biochim. Biophys. Acta (2015), http://dx.doi.org/10.1016/j.bbagen.2015.12.016

in cellular adherence and signaling were affected by this altered glycosylation. Important targets included key players in malignancy, such as integrins, which are known to mediate the interaction of cancer cells to the extracellular matrix [33]. Integrin glycosylation has been shown to modulate the cell adhesion to fibronectin and to affect cancer cell invasion and metastasis [65].

In this study we only considered for validation unique peptide sequences that contained *N*-glycosylation sites. The majority of enriched peptides, due to increased sialylation on *O*-glycans or due to common amino acid sequences, were excluded from the analysis. With our approach we could not distinguish between sialic acid linkage and therefore the generation of information of glycopeptides with specific increases of α2-3 sialic acids was precluded. Nonetheless, our approach allowed to identify numerous targets showing altered glycosylation that can be used for follow-up studies. Further, it illustrates that alterations of a single glycosyltransferase can affect a multitude of cancer relevant targets.

4.3. Receptor glycosylation as a modulator of activity in cancer

Receptor tyrosine kinases are glycoproteins and key players of transformation and malignant growth [66]. Glycosylation alterations have been demonstrated to modulate receptor activity [24,67,68]. In the present study we have focused on the alterations leading to the receptor RON activation. In the last years several efforts have been made to target RON in cancer patients. Currently several tyrosine kinase inhibitors and monoclonal antibodies against RON are applied in clinical or pre-clinical trials for therapeutic efficacy [69–76]. Our screening revealed that this receptor, which has been described to be an oncogene in gastric cancer [12], showed an altered glycosylation and concomitant increased activation. RON presents 3 immunoglobulin-like plexin and transcription (IPT) domains that have been described as a cause for constitutive activation in cancer when altered [39,77]. We demonstrated that Asn841 shows increased sialylation in cells overexpressing ST3GAL4 (Table 5 in [25]). The Asn841 is located in one of the IPT domains and therefore may underlie the increased activation of this cellular RTK. Further analysis by proximity ligation assay confirmed the glycosylation of RON with SLe^X in human gastric carcinoma tissues. These observations support that the altered glycosylation observed in this receptor in gastric cancer may lead to its dysfunctional oncogenic activation and therefore modulating the more aggressive cancer phenotype associated with SLe^X expressing tumors. Further studies are warranted to evaluate the biomarker potential of RON glycosylation profile for gastric cancer staging, prognosis and therapeutic response.

4.4. Potential application in cancer therapy and future outlook

Hyper-activation of RTKs due to their upregulation or mutations are common oncogenic events that modern medicine tries to evaluate in the process of tumor screening to design a personalized treatment via inhibitors [9]. However, the present screening methods mostly rely on identifying mutations or gene amplifications [78,79], and therefore, are not considering post-translational modifications, such as glycosylation, as potential activators in a cancer context. We demonstrated in this work that aberrant glycosylation is an alternative route of RTK activation in cancer, emphasizing the necessity for its evaluation in tumor characterization and patient profiling.

A common drawback of whole glycome analysis is its intrinsic complexity, delaying its application in the clinical routine. Much has to be done to simplify and standardize such glycome analysis and to improve our understanding of glycosylation alterations on specific targets. However, the present work demonstrates the importance of such approaches in addressing complex diseases in combination with large scale genomics, transcriptomics and proteomics. We are convinced that the screening of specific target proteins for glycan alterations can be a future corner stone of clinical tumor characterization complementing the conventional methods and therefore leading to improved molecular characterization of cancers for a better diagnosis, prognosis and therapeutics.

Transparency document

The Transparency document is associated with this article can be found, in the online version.

Acknowledgements

We acknowledge the support from the European Union, Seventh Framework Programme, Gastric Glyco Explorer initial training network: grant number 316929. IPATIMUP integrates the i3S Research Unit, which is partially supported by FCT, the Portuguese Foundation for Science and Technology. This work is funded by FEDER funds through the Operational Programme for Competitiveness Factors-COMPETE (FCOMP-01-0124-FEDER028188) and National Funds through the FCT-Foundation for Science and Technology, under the projects: PEst-C/SAU/LA0003/2013, PTDC/BBB-EBI/0786/2012, and PTDC/BBB-EBI/0567/2014 (to CAR). This work was also supported by "Glycoproteomics" project grant number PCIG09-GA-2011-293847 (to DK) and the Danish Natural Science Research Council and a generous grant from the VILLUM Foundation to the VILLUM Center for Bioanalytical Sciences at the University of Southern Denmark (to MRL). Grants were received from FCT, POPH (Programa Operacional Potencial Humano) and FSE (Fundo Social Europeu): SFRH/BPD/75871/2011 to AM; SFRH/BPD/111048/2015 to JAF; SFRH/BPD/96510/2013 to CG. The UPLC instrument was obtained with a grant from the Ingabritt and Arne Lundbergs Research Foundation (to NK). C.J. was supported by the Knut and Alice Wallenberg Foundation. The mass spectrometer (LTQ) was obtained by a grant from the Swedish Research Council (342-2004-4434) (to NK).

Appendix A. Supplementary data

Supplementary data to this article can be found online at http://dx.doi.org/10.1016/j.bbagen.2015.12.016.

References

[1] R.L. Siegel, K.D. Miller, A. Jemal, Cancer statistics, 2015, CA Cancer J. Clin. 65 (2015) 5–29.
[2] M. May, Statistics: attacking an epidemic, Nature 509 (2014) S50–S51.
[3] J. Ferlay, E. Steliarova-Foucher, J. Lortet-Tieulent, S. Rosso, J.W. Coebergh, H. Comber, D. Forman, F. Bray, Cancer incidence and mortality patterns in Europe: estimates for 40 countries in 2012, Eur. J. Cancer 49 (2013) 1374–1403.
[4] M. Carpelan-Holmstrom, J. Louhimo, U.H. Stenman, H. Alfthan, C. Haglund, CEA, CA 19-9 and CA 72-4 improve the diagnostic accuracy in gastrointestinal cancers, Anticancer Res. 22 (2002) 2311–2316.
[5] C.A. Reis, H. Osorio, L. Silva, C. Gomes, L. David, Alterations in glycosylation as biomarkers for cancer detection, J. Clin. Pathol. 63 (2010) 322–329.
[6] A. Varki, R. Kannagi, B.P. Toole, Glycosylation Changes in Cancer, in: A. Varki, R.D. Cummings, J.D. Esko, H.H. Freeze, P. Stanley, C.R. Bertozzi, G.W. Hart, M.E. Etzler (Eds.), Essentials of Glycobiology, Cold Spring Harbor, NY, 2009.
[7] S.S. Pinho, C.A. Reis, Glycosylation in cancer: mechanisms and clinical implications, Nat. Rev. Cancer 15 (2015) 540–555.
[8] K.M. Wong, T.J. Hudson, J.D. McPherson, Unraveling the genetics of cancer: genome sequencing and beyond, Annu. Rev. Genomics Hum. Genet. 12 (2011) 407–430.
[9] R.L. Schilsky, Personalized medicine in oncology: the future is now, Nat. Rev. Drug Discov. 9 (2010) 363–366.
[10] C. Sawyers, Targeted cancer therapy, Nature 432 (2004) 294–297.
[11] A. Arora, E.M. Scholar, Role of tyrosine kinase inhibitors in cancer therapy, J. Pharmacol. Exp. Ther. 315 (2005) 971–979.
[12] H.P. Yao, Y.Q. Zhou, R. Zhang, M.H. Wang, MSP-RON signalling in cancer: pathogenesis and therapeutic potential, Nat. Rev. Cancer 13 (2013) 466–481.
[13] A.S. Carvalho, A. Harduin-Lepers, A. Magalhaes, E. Machado, N. Mendes, L.T. Costa, R. Matthiesen, R. Almeida, J. Costa, C.A. Reis, Differential expression of alpha-2,3-sialyltransferases and alpha-1,3/4-fucosyltransferases regulates the levels of sialyl Lewis a and sialyl Lewis x in gastrointestinal carcinoma cells, Int. J. Biochem. Cell Biol. 42 (2010) 80–89.
[14] T. Conze, A.S. Carvalho, U. Landegren, R. Almeida, C.A. Reis, L. David, O. Soderberg, MUC2 mucin is a major carrier of the cancer-associated sialyl-Tn antigen in intestinal metaplasia and gastric carcinomas, Glycobiology 20 (2010) 199–206.

[15] P. Lauren, The two histological main types of gastric carcinoma: diffuse and so-called intestinal-type carcinoma. An attempt at a histo-clinical classification, Acta Pathol. Microbiol. Scand. 64 (1965) 31–49.
[16] B.L. Schulz, N.H. Packer, N.G. Karlsson, Small-scale analysis of O-linked oligosaccharides from glycoproteins and mucins separated by gel electrophoresis, Anal. Chem. 74 (2002) 6088–6097.
[17] L. Royle, C.M. Radcliffe, R.A. Dwek, P.M. Rudd, Detailed structural analysis of N-glycans released from glycoproteins in SDS-PAGE gel bands using HPLC combined with exoglycosidase array digestions, Methods Mol. Biol. 347 (2006) 125–143.
[18] K. Engholm-Keller, P. Birck, J. Storling, F. Pociot, T. Mandrup-Poulsen, M.R. Larsen, TiSH—a robust and sensitive global phosphoproteomics strategy employing a combination of TiO_2, SIMAC, and HILIC, J. Proteomics 75 (2012) 5749–5761.
[19] M.N. Melo-Braga, M. Ibanez-Vea, M.R. Larsen, K. Kulej, Comprehensive protocol to simultaneously study protein phosphorylation, acetylation, and N-linked sialylated glycosylation, Methods Mol. Biol. 1295 (2015) 275–292.
[20] V. Schwammle, I.R. Leon, O.N. Jensen, Assessment and improvement of statistical tools for comparative proteomics analysis of sparse data sets with few experimental replicates, J. Proteome Res. 12 (2013) 3874–3883.
[21] A. Harduin-Lepers, M.A. Krzewinski-Recchi, F. Colomb, F. Foulquier, S. Groux-Degroote, P. Delannoy, Sialyltransferases functions in cancers, Front. Biosci. 4 (2012) 499–515.
[22] K. Sasaki, E. Watanabe, K. Kawashima, S. Sekine, T. Dohi, M. Oshima, N. Hanai, T. Nishi, M. Hasegawa, Expression cloning of a novel Gal beta (1-3/1-4) GlcNAc alpha 2,3-sialyltransferase using lectin resistance selection, J. Biol. Chem. 268 (1993) 22782–22787.
[23] H. Kitagawa, J.C. Paulson, Cloning of a novel alpha 2,3-sialyltransferase that sialylates glycoprotein and glycolipid carbohydrate groups, J. Biol. Chem. 269 (1994) 1394–1401.
[24] C. Gomes, H. Osorio, M.T. Pinto, D. Campos, M.J. Oliveira, C.A. Reis, Expression of ST3GAL4 leads to SLe(x) expression and induces c-Met activation and an invasive phenotype in gastric carcinoma cells, PLoS One 8 (2013), e66737.
[25] S. Mereiter, A. Magalhães, B. Adamczyk, C. Jin, A. Almeida, L. Drici, M. Ibanez-Vea, M.R. Larsen, D. Kolarich, N.G. Karlsson, C.A. Reis, Glycomic and sialoproteomic data of gastric carcinoma cells overexpressing ST3GAL4, Data in Brief (2015) (submitted for publication).
[26] A. Ishizuka, Y. Hashimto, R. Naka, M. Kinoshita, K. Kakehi, J. Seino, Y. Funakoshi, T. Suzuki, A. Kameyama, H. Narimatsu, Accumulation of free complex-type N-glycans in MKN7 and MKN45 stomach cancer cells, Biochem. J. 413 (2008) 227–237.
[27] S.S. Pinho, C.A. Reis, J. Paredes, A.M. Magalhaes, A.C. Ferreira, J. Figueiredo, W. Xiaogang, F. Carneiro, F. Gartner, R. Seruca, The role of N-acetylglucosaminyltransferase III and V in the post-transcriptional modifications of E-cadherin, Hum. Mol. Genet. 18 (2009) 2599–2608.
[28] Y. Zhao, T. Nakagawa, S. Itoh, K. Inamori, T. Isaji, Y. Kariya, A. Kondo, E. Miyoshi, K. Miyazaki, N. Kawasaki, N. Taniguchi, J. Gu, N-acetylglucosaminyltransferase III antagonizes the effect of N-acetylglucosaminyltransferase V on alpha3beta1 integrin-mediated cell migration, J. Biol. Chem. 281 (2006) 32122–32130.
[29] M.R. Kudelka, T. Ju, J. Heimburg-Molinaro, R.D. Cummings, Simple sugars to complex disease—mucin-type O-glycans in cancer, Adv. Cancer Res. 126 (2015) 53–135.
[30] Y. Rossez, E. Maes, T. Lefebvre Darroman, P. Gosset, C. Ecobichon, M. Joncquel Chevalier Curt, I.G. Boneca, J.C. Michalski, C. Robbe-Masselot, Almost all human gastric mucin O-glycans harbor blood group A, B or H antigens and are potential binding sites for Helicobacter pylori, Glycobiology 22 (2012) 1193–1206.
[31] C. Boccaccio, P.M. Comoglio, Invasive growth: a MET-driven genetic programme for cancer and stem cells, Nat. Rev. Cancer 6 (2006) 637–645.
[32] N. Beauchemin, A. Arabzadeh, Carcinoembryonic antigen-related cell adhesion molecules (CEACAMs) in cancer progression and metastasis, Cancer Metastasis Rev. 32 (2013) 643–671.
[33] J.S. Desgrosellier, D.A. Cheresh, Integrins in cancer: biological implications and therapeutic opportunities, Nat. Rev. Cancer 10 (2010) 9–22.
[34] M.H. Wang, W. Lee, Y.L. Luo, M.T. Weis, H.P. Yao, Altered expression of the RON receptor tyrosine kinase in various epithelial cancers and its contribution to tumourigenic phenotypes in thyroid cancer cells, J. Pathol. 213 (2007) 402–411.
[35] M.N. Thobe, D. Gurusamy, P. Pathrose, S.E. Waltz, The Ron receptor tyrosine kinase positively regulates angiogenic chemokine production in prostate cancer cells, Oncogene 29 (2010) 214–226.
[36] J. Logan-Collins, R.M. Thomas, P. Yu, D. Jaquish, E. Mose, R. French, W. Stuart, R. McClaine, B. Aronow, R.M. Hoffman, S.E. Waltz, A.M. Lowy, Silencing of RON receptor signaling promotes apoptosis and gemcitabine sensitivity in pancreatic cancers, Cancer Res. 70 (2010) 1130–1140.
[37] R.J. McClaine, A.M. Marshall, P.K. Wagh, S.E. Waltz, Ron receptor tyrosine kinase activation confers resistance to tamoxifen in breast cancer cell lines, Neoplasia 12 (2010) 650–658.
[38] D.V. Catenacci, G. Cervantes, S. Yala, E.A. Nelson, E. El-Hashani, R. Kanteti, M. El Dinali, R. Hasina, J. Bragelmann, T. Seiwert, M. Sanicola, L. Henderson, T.A. Grushko, O. Olopade, T. Karrison, Y.J. Bang, W.H. Kim, M. Tretiakova, E. Vokes, D.A. Frank, H.L. Kindler, H. Huet, R. Salgia, RON (MST1R) is a novel prognostic marker and therapeutic target for gastro-esophageal adenocarcinoma, Cancer Biol. Ther. 12 (2011) 9–46.
[39] C. Collesi, M.M. Santoro, G. Gaudino, P.M. Comoglio, A splicing variant of the RON transcript induces constitutive tyrosine kinase activity and an invasive phenotype, Mol. Cell. Biol. 16 (1996) 5518–5526.
[40] M.M. Santoro, C. Collesi, S. Grisendi, G. Gaudino, P.M. Comoglio, Constitutive activation of the RON gene promotes invasive growth but not transformation, Mol. Cell. Biol. 16 (1996) 7072–7083.
[41] M. Amado, F. Carneiro, M. Seixas, H. Clausen, M. Sobrinho-Simoes, Dimeric sialyl-Le(x) expression in gastric carcinoma correlates with venous invasion and poor outcome, Gastroenterology 114 (1998) 462–470.
[42] R. Kannagi, Carbohydrate-mediated cell adhesion involved in hematogenous metastasis of cancer, Glycoconj. J. 14 (1997) 577–584.
[43] S. Nakamori, M. Kameyama, S. Imaoka, H. Furukawa, O. Ishikawa, Y. Sasaki, Y. Izumi, T. Irimura, Involvement of carbohydrate antigen sialyl Lewis(x) in colorectal cancer metastasis, Dis. Colon Rectum 40 (1997) 420–431.
[44] M. Tatsumi, A. Watanabe, H. Sawada, Y. Yamada, Y. Shino, H. Nakano, Immunohistochemical expression of the sialyl Lewis x antigen on gastric cancer cells correlates with the presence of liver metastasis, Clin. Exp. Metastasis 16 (1998) 743–750.
[45] S.E. Baldus, T.K. Zirbes, S.P. Monig, S. Engel, E. Monaca, K. Rafiqpoor, F.G. Hanisch, C. Hanski, J. Thiele, H. Pichlmaier, H.P. Dienes, Histopathological subtypes and prognosis of gastric cancer are correlated with the expression of mucin-associated sialylated antigens: sialosyl-Lewis(a), sialosyl-Lewis(x) and sialosyl-Tn, Tumour Biol. 19 (1998) 445–453.
[46] M. Perez-Garay, B. Arteta, E. Llop, L. Cobler, L. Pages, R. Ortiz, M.J. Ferri, C. de Bolos, J. Figueras, R. de Llorens, F. Vidal-Vanaclocha, R. Peracaula, alpha2,3-Sialyltransferase ST3Gal IV promotes migration and metastasis in pancreatic adenocarcinoma cells and tends to be highly expressed in pancreatic adenocarcinoma tissues, Int. J. Biochem. Cell Biol. 45 (2013) (1748-1757).
[47] Y.J. Kim, A. Varki, Perspectives on the significance of altered glycosylation of glycoproteins in cancer, Glycoconj. J. 14 (1997) 569–576.
[48] F. Dall'Olio, M. Chiricolo, Sialyltransferases in cancer, Glycoconj. J. 18 (2001) 841–850.
[49] S. Lin, W. Kemmner, S. Grigull, P.M. Schlag, Cell surface alpha 2,6 sialylation affects adhesion of breast carcinoma cells, Exp. Cell Res. 276 (2002) 101–110.
[50] H. Yamamoto, A. Oviedo, C. Sweeley, T. Saito, J.R. Moskal, Alpha2,6-sialylation of cell-surface N-glycans inhibits glioma formation in vivo, Cancer Res. 61 (2001) 6822–6829.
[51] M. Chiricolo, N. Malagolini, S. Bonfiglioli, F. Dall'Olio, Phenotypic changes induced by expression of beta-galactoside alpha2,6 sialyltransferase I in the human colon cancer cell line SW948, Glycobiology 16 (2006) 146–154.
[52] R. Kornfeld, S. Kornfeld, Assembly of asparagine-linked oligosaccharides, Annu. Rev. Biochem. 54 (1985) 631–664.
[53] N. Taniguchi, Y. Ihara, Recent progress in the molecular biology of the cloned N-acetylglucosaminyltransferases, Glycoconj. J. 12 (1995) 733–738.
[54] S. Kellokumpu, R. Sormunen, I. Kellokumpu, Abnormal glycosylation and altered Golgi structure in colorectal cancer: dependence on intra-Golgi pH, FEBS Lett. 516 (2002) 217–224.
[55] Y. Song, J.A. Aglipay, J.D. Bernstein, S. Goswami, P. Stanley, The bisecting GlcNAc on N-glycans inhibits growth factor signaling and retards mammary tumor progression, Cancer Res. 70 (2010) 3361–3371.
[56] S.S. Pinho, P. Oliveira, J. Cabral, S. Carvalho, D. Huntsman, F. Gartner, R. Seruca, C.A. Reis, C. Oliveira, Loss and recovery of Mgat3 and GnT-III Mediated E-cadherin N-glycosylation is a mechanism involved in epithelial-mesenchymal–epithelial transitions, PLoS One 7 (2012), e33191.
[57] S. Hakomori, Aberrant glycosylation in tumors and tumor-associated carbohydrate antigens, Adv. Cancer Res. 52 (1989) 257–331.
[58] P.H. Jensen, N.G. Karlsson, D. Kolarich, N.H. Packer, Structural analysis of N- and O-glycans released from glycoproteins, Nat. Protoc. 7 (2012) 1299–1310.
[59] D. Kolarich, M. Windwarder, K. Alagesan, F. Altmann, Isomer-specific analysis of released N-glycans by LC-ESI MS/MS with porous graphitized carbon, Methods Mol. Biol. 1321 (2015) 427–435.
[60] C. Slawson, G.W. Hart, O-GlcNAc signalling: implications for cancer cell biology, Nat. Rev. Cancer 11 (2011) 678–684.
[61] F. Alisson-Silva, L. Freire-de-Lima, J.L. Donadio, M.C. Lucena, L. Penha, J.N. Sa-Diniz, W.B. Dias, A.R. Todeschini, Increase of O-glycosylated oncofetal fibronectin in high glucose-induced epithelial–mesenchymal transition of cultured human epithelial cells, PLoS One 8 (2013), e60471.
[62] S. Olivier-Van Stichelen, C. Guinez, A.M. Mir, Y. Perez-Cervera, C. Liu, J.C. Michalski, T. Lefebvre, The hexosamine biosynthetic pathway and O-GlcNAcylation drive the expression of beta-catenin and cell proliferation, Am. J. Physiol. Endocrinol. Metab. 302 (2012) E417–E424.
[63] Z. Ma, D.J. Vocadlo, K. Vosseller, Hyper-O-GlcNAcylation is anti-apoptotic and maintains constitutive NF-kappaB activity in pancreatic cancer cells, J. Biol. Chem. 288 (2013) 15121–15130.
[64] P. Stanley, Golgi Glycosylation, Cold Spring Harbor Perspectives In Biology, 3, 2011.
[65] J. Gu, N. Taniguchi, Regulation of integrin functions by N-glycans, Glycoconj. J. 21 (2004) 9–15.
[66] D. Hanahan, R.A. Weinberg, Hallmarks of cancer: the next generation, Cell 144 (2011) 646–674.
[67] K. Kaszuba, M. Grzybek, A. Orlowski, R. Danne, T. Rog, K. Simons, U. Coskun, I. Vattulainen, N-Glycosylation as determinant of epidermal growth factor receptor conformation in membranes, Proc. Natl. Acad. Sci. U. S. A. 112 (2015) 4334–4339.
[68] A. Cazet, S. Julien, M. Bobowski, J. Burchell, P. Delannoy, Tumour-associated carbohydrate antigens in breast cancer, Breast Cancer Res. 12 (2010) 204.
[69] T.K. Choueiri, U. Vaishampayan, J.E. Rosenberg, T.F. Logan, A.L. Harzstark, R.M. Bukowski, B.I. Rini, S. Srinivas, M.N. Stein, L.M. Adams, L.H. Ottesen, K.H. Laubscher, L. Sherman, D.F. McDermott, N.B. Haas, K.T. Flaherty, R. Ross, P. Eisenberg, P.S. Meltzer, M.J. Merino, D.P. Bottaro, W.M. Linehan, R. Srinivasan, Phase II and biomarker study of the dual MET/VEGFR2 inhibitor foretinib in patients with papillary renal cell carcinoma, J. Clin. Oncol. 31 (2013) 181–186.
[70] A. Belalcazar, D. Azana, C.A. Perez, L.E. Raez, E.S. Santos, Targeting the Met pathway in lung cancer, Expert. Rev. Anticancer. Ther. 12 (2012) 519–528.
[71] Y. Zhang, P.J. Kaplan-Lefko, K. Rex, Y. Yang, J. Moriguchi, T. Osgood, B. Mattson, A. Coxon, M. Reese, T.S. Kim, J. Lin, A. Chen, T.L. Burgess, I. Dussault, Identification of a novel recepteur d'origine nantais/c-met small-molecule kinase inhibitor with antitumor activity in vivo, Cancer Res. 68 (2008) 6680–6687.
[72] S. Sharma, J.Y. Zeng, C.M. Zhuang, Y.Q. Zhou, H.P. Yao, X. Hu, R. Zhang, M.H. Wang, Small-molecule inhibitor BMS-777607 induces breast cancer cell polyploidy with increased resistance to cytotoxic chemotherapy agents, Mol. Cancer Ther. 12 (2013) 725–736.

Please cite this article as: S. Mereiter, et al., Glycomic analysis of gastric carcinoma cells discloses glycans as modulators of RON receptor tyrosine kinase activation in cancer, Biochim. Biophys. Acta (2015), http://dx.doi.org/10.1016/j.bbagen.2015.12.016

[73] B.S. Pan, G.K. Chan, M. Chenard, A. Chi, L.J. Davis, S.V. Deshmukh, J.B. Gibbs, S. Gil, G. Hang, H. Hatch, J.P. Jewell, I. Kariv, J.D. Katz, K. Kunii, W. Lu, B.A. Lutterbach, C.P. Paweletz, X. Qu, J.F. Reilly, A.A. Szewczak, Q. Zeng, N.E. Kohl, C.J. Dinsmore, MK-2461, a novel multitargeted kinase inhibitor, preferentially inhibits the activated c-Met receptor, Cancer Res. 70 (2010) 1524–1533.

[74] A.B. Northrup, M.H. Katcher, M.D. Altman, M. Chenard, M.H. Daniels, S.V. Deshmukh, D. Falcone, D.J. Guerin, H. Hatch, C. Li, W. Lu, B. Lutterbach, T.J. Allison, S.B. Patel, J.F. Reilly, M. Reutershan, K.W. Rickert, C. Rosenstein, S.M. Soisson, A.A. Szewczak, D. Walker, K. Wilson, J.R. Young, B.S. Pan, C.J. Dinsmore, Discovery of 1-[3-(1-methyl-1H-pyrazol-4-yl)-5-oxo-5H-benzo[4,5]cyclohepta[1,2-b]pyridin-7-yl]-N-(pyridin-2-ylmethyl)methanesulfonamide (MK-8033): a specific c-Met/Ron dual kinase inhibitor with preferential affinity for the activated state of c-Met, J. Med. Chem. 56 (2013) 2294–2310.

[75] J.M. O'Toole, K.E. Rabenau, K. Burns, D. Lu, V. Mangalampalli, P. Balderes, N. Covino, R. Bassi, M. Prewett, K.J. Gottfredsen, M.N. Thobe, Y. Cheng, Y. Li, D.J. Hicklin, Z. Zhu, S.E. Waltz, M.J. Hayman, D.L. Ludwig, D.S. Pereira, Therapeutic implications of a human neutralizing antibody to the macrophage-stimulating protein receptor tyrosine kinase (RON), a c-MET family member, Cancer Res. 66 (2006) 9162–9170.

[76] Z. Gunes, A. Zucconi, M. Cioce, A. Meola, M. Pezzanera, S. Acali, I. Zampaglione, V. De Pratti, L. Bova, F. Talamo, A. Demartis, P. Monaci, N. La Monica, G. Ciliberto, A. Vitelli, Isolation of fully human antagonistic RON antibodies showing efficient block of downstream signaling and cell migration, Transl. Oncol. 4 (2011) 38–46.

[77] Q. Ma, K. Zhang, S. Guin, Y.Q. Zhou, M.H. Wang, Deletion or insertion in the first immunoglobulin-plexin-transcription (IPT) domain differentially regulates expression and tumorigenic activities of RON receptor tyrosine kinase, Mol. Cancer 9 (2010) 307.

[78] M. Ingelman-Sundberg, Personalized medicine into the next generation, J. Intern. Med. 277 (2015) 152–154.

[79] T. Tursz, R. Bernards, Hurdles on the road to personalized medicine, Mol. Oncol. 9 (2015) 935–939.

[80] N. Shibuya, I.J. Goldstein, W.F. Broekaert, M. Nsimba-Lubaki, B. Peeters, W.J. Peumans, The elderberry (*Sambucus nigra* L.) bark lectin recognizes the Neu5Ac(alpha 2-6)Gal/GalNAc sequence, J. Biol. Chem. 262 (1987) 1596–1601.

Please cite this article as: S. Mereiter, et al., Glycomic analysis of gastric carcinoma cells discloses glycans as modulators of RON receptor tyrosine kinase activation in cancer, Biochim. Biophys. Acta (2015), http://dx.doi.org/10.1016/j.bbagen.2015.12.016